Leadership in Sustainable Infrastructure

Leadership en Infrastructures Durables

Vancouver, Canada

May 31 – June 3, 2017/ *Mai 31 – Juin 3, 2017*

OBSERVATION OF POLYMER MODIFIED ASPHALT MICROSTRUCTURE BY ESEM

Peter Mikhailenko [1,5], Changjiang Kou [2], Hassan Baaj [3], and Susan Tighe[4]

[1] Centre for Pavement and Transportation Technology, Department of Civil and Environmental Engineering, Faculty of Engineering, University of Waterloo, Canada

[2] Institute of Road and Transportation Engineering, College of Civil Science and Engineering, Yangzhou University, China; Centre for Pavement and Transportation Technology, Department of Civil and Environmental Engineering, Faculty of Engineering, University of Waterloo, Canada

[3] Centre for Pavement and Transportation Technology, Department of Civil and Environmental Engineering, Faculty of Engineering, University of Waterloo, Canada

[4] Centre for Pavement and Transportation Technology, Department of Civil and Environmental Engineering, Faculty of Engineering, University of Waterloo, Canada

[5] p2mikhai@uwaterloo.ca

ABSTRACT

The observation of asphalt binder microstructure with the Environmental Scanning Electron Microscope (ESEM) has yielded promising results. There have been findings that show the microstructure evolving with aging and certain loading applications. The goal of this study was to observe the PMA microstructure using ESEM analysis. Four PMA binders of varying PG grades were observed in ESEM, comparing them to a straight run binder. The binders were compared in terms of the fibril diameter and shape observed visually, along with the fibril structure. The initial 'bee' structures before the appearance of the fibrils were also compared. It was found that the PMA binders had a denser fibril structure, corresponding to their higher PG grades indicating stiffer binders, although this varied with different PMAs. The images were also analyzed by calculating the area and length of the fibrils through an image analysis protocol. This study is a step towards the further understanding of the microstructure of PMAs.

Keywords: - asphalt binder testing, polymer modified, PMA, ESEM, microscopy

1. INTRODUCTION

Advances in polymer technology and its descending cost has opened the possibility for its use in asphalt pavement, particularly with regards to the asphalt binder. Asphalt binder combined with polymers, or Polymer Modified Asphalt (PMA), has been patented as early as 1843, with test projects starting in Europe in the 1930s and North America in the 1950s (Yildirim, 2007). A number of polymers are in wide use today, including styrene–butadiene rubber (SBR), styrene–butadiene block (SBS) and ethylene/vinyl acetate (EVA) copolymers (Cortizo et al., 2004). These polymers can be added to modify the thermal and performance properties of the asphalt binder, improving the binder performance in both cold and hot environments, improving (Becker et al., 2001), Additionally, it allows for the reduction of thermal energy used in the mixing process, as in the case of warm or cold mix asphalt (Mazumder et al., 2016), thus, improving the pavement's ecological footprint. With the increasing use of PMA over the past few decades, there is a need for both research on PMA and proper quality control and quality assurance (QC/QA) (Yildirim, 2007). There is the added challenge from the fact that PMA will add additional variability to the

recovered pavement, which is especially important to understand in the case of Reclaimed Asphalt Pavement (RAP) (Baghaee Moghaddam and Baaj, 2016).

There are a number of techniques used to analyze asphalt binder microstructure. This has produced studies looking at PMAs specifically, with techniques such as optical microscopy (Dehouche et al., 2012; Garcia-Morales et al., 2006), atomic force microscopy (AFM; (Tarefder and Arifuzzaman, 2011), fluorescence microscopy (Kou et al., 2015) and infrared microscopy (Mouillet et al., 2008). Another promising technique for observing asphalt microstructure is Environmental Scanning Electron Microscopy (ESEM). The electron beam emitted by the ESEM displaces of the lighter binder molecules, revealing a microstructure, which has been shown to correspond to the resins and possibly a part of the asphaltenes fraction of the binder (Gaskin, 2013). The microstructure has been found to evolve with both binder aging and tensile forces (Rozeveld et al., 1997). It has been used to analyze asphalt binders without the risks involved in damaging the apparatus, as can be the case with the Scanning Electron Microscope (SEM) (Mikhailenko, 2015). The pumps of the ESEM are designed to handle volatile organic compounds with limited risk of them clogging them up and damaging the apparatus (Danilatos, 1993).

The objective of the current study is the analysis of PMA microstructure with ESEM. One straight run binder and 4 PMAs were observed for this study. Firstly, the microstructure of PMA binders was analyzed with the ESEM, in terms of how it developed during observation and the resulting microstructure. The straight run binder was compared to the PMAs, and the characteristics of the PMAs in the ESEM image were identified. Secondly, the images were analyzed through an image analysis protocol by calculating the area and length of the fibrils. The results of this study will be used as a step toward the better understanding of PMA microstructure.

2. MATERIALS AND METHODS

2.1 Asphalt Binder

One straight run and four polymer modified asphalts were used in this study. The straight run binder had a PG grade of 58-28. The same 58-28 binder was modified by mixing it with 10%w (Styrene/Butadiene/Styrene) SBS polymer. The three other PMAs had PG grades of 76-28. 82-28 and 88-28, giving us a wide range of PMA modification.

2.2 Sample Preparation

For the ESEM observation, a stainless steel mould was prepared (Mikhailenko et al., 2016), with a cylindrical opening of 8 mm in diameter and 2 mm in height. The square perimeter of the mould was 10x10 mm and a 15 mm long handle was also added to be able to move it safely, with a 5 mm long base to ensure that the mould did not tip over (Figure 1).

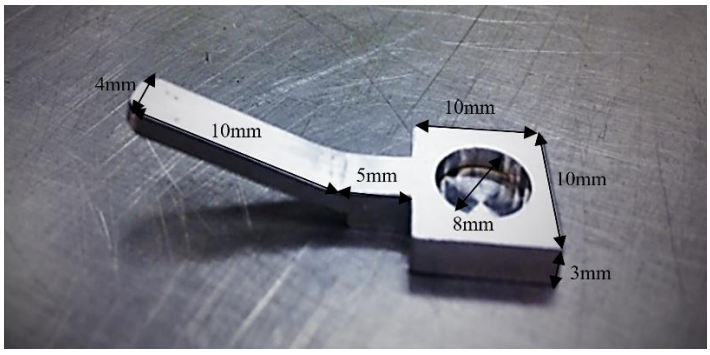

Figure 1 Stainless Steel Sample Mould

The binders were softened by placing them inside covered containers and heating them in an oven for approximately 1h at 110°C and 1h at 150°C for the four PMAs, which were stiffer and needed more energy to liquefy enough to sample. Approximately 0.1 g was subsequently poured from the containers into the sample holders using a spatula and flattening the sample the same by holding the sample holder on a hotplate at 150°C for approximately 10s for the virgin binder and up to 30s for the stiffer PMAs. The samples were stored in a cooler at 6°C overnight before the test.

2.3 ESEM Observation

The observations (Figure 2) were conducted at room temperature immediately after being removed from the cooler with a FEI Quanta 250 FEG ESEM. The observation parameters were an acceleration voltage of 20 keV, a spot size of 3.5 and a chamber pressure of 0.8 mbar in low vacuum mode, and a magnification of 1000x in secondary electron (SE) mode, in accordance with the settings developed previously for ESEM observation of asphalt binder (Mikhailenko et al., 2016). The electron gun was kept at a distance of 15 mm from the surface of the sample.

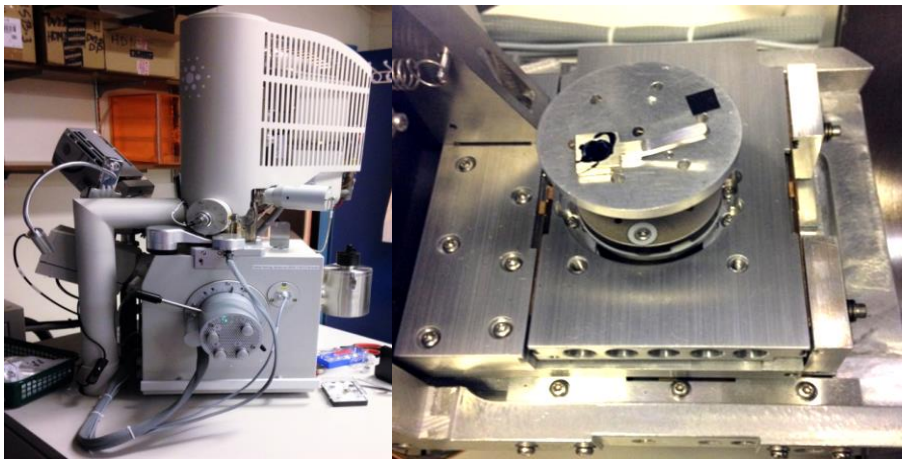

Figure 2 ESEM Apparatus (left) and Sample in the ESEM Stage (right)

3. RESULTS AND DISCUSSION

3.1 Polymer Modified Asphalt under ESEM

As mentioned previously, the ESEM image evolves from the time it is subjected to the electron beam. The image evolves from flat and dark, sometimes with observable micelle structure, to a three-dimensional fibril microstructure. The characteristics of the structures in these images were analyzed, along with the time it takes for them to form.
In the current analysis, both the initial and "stabilized" images from the ESEM observation have been be presented. The initial images show the surface properties of the binder before the electron beam irradiates the surface, which has been shown to reveal a 'bee' structure while the final, stabilized images show the 3D fibril microstructure of the binder (Mikhailenko et al., 2016). Both these images are shown side by side in the following figures.

The straight-run binder (Figure 3) initially revealed a 'bee' structure with fairly densely packed 'bee-like' shapes, similar to the one observed with AFM (Das et al., 2015). This evolved into a fairly loose and smooth fibril structure typical of the ones found in unaged straight-run binder (Mikhailenko et al., 2016). The same binder with 10% added SBS polymer showed some significant differences (Figure 4). The initial 'bee' structure appears to have remained for this binder, with the addition of 2-10 µm circular particles, which were identified as SBS, corresponding to the SBS observed in SEM from previous studies (Puente-Lee et al., 2003). The fibril structure became somewhat denser and more connected with the addition of SBS, corresponding to a stiffer binder that would be expected with SBS addition (Navarro et al., 2005).

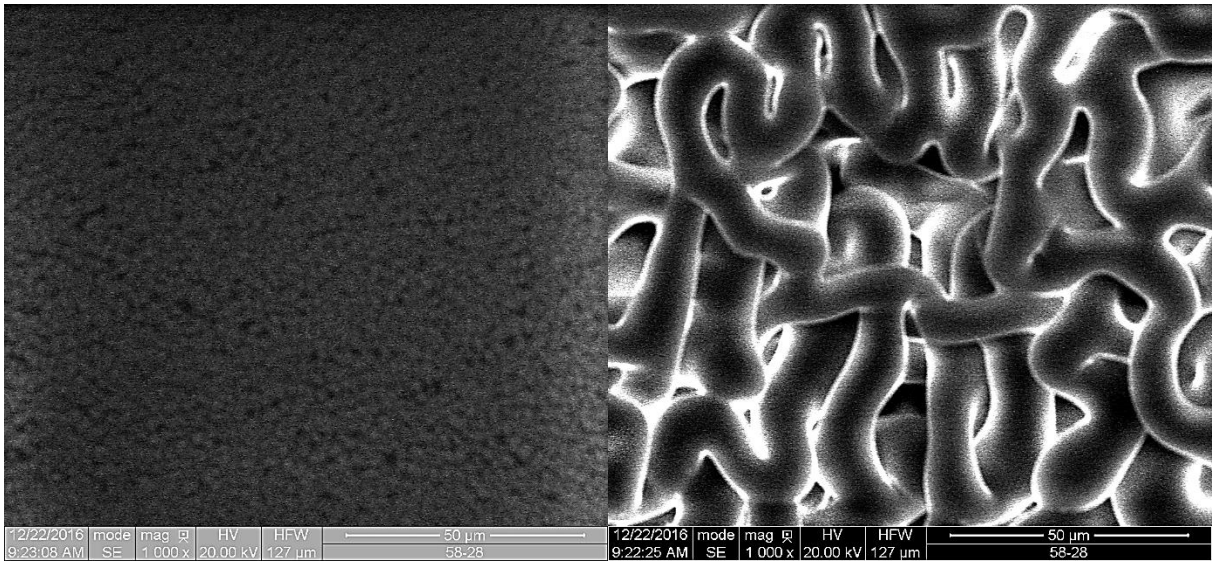

Figure 3 ESEM Images for 58-28 Straight-Run Binder before (left) and after (right) Electron Beam Irradiation

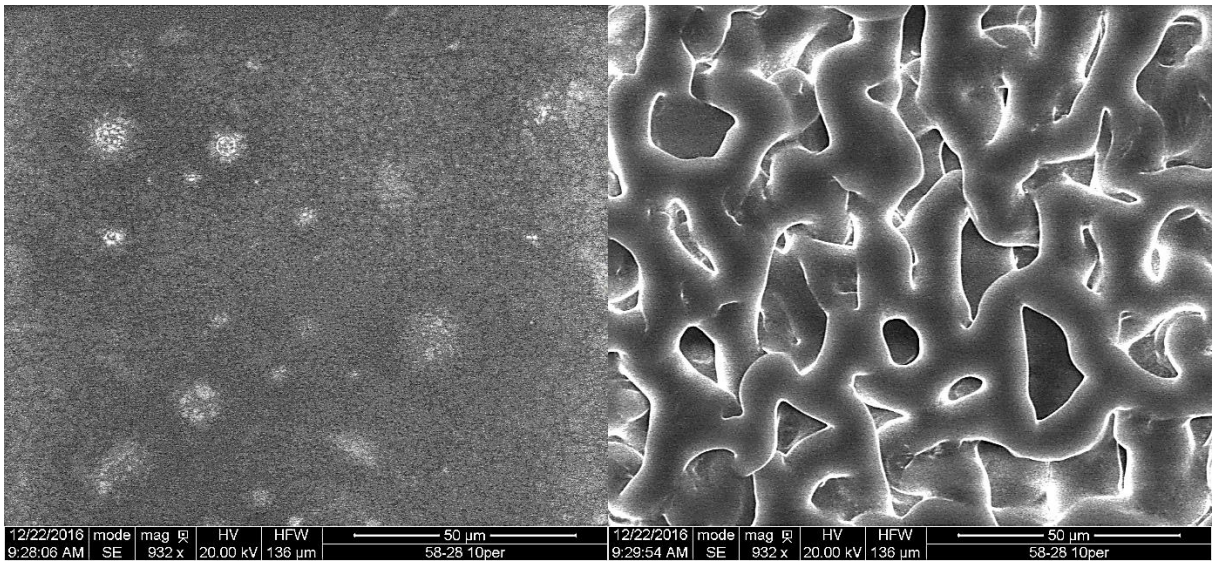

Figure 4 ESEM Images for 58-28 + 10% SBS Binder before (left) and after (right) Electron Beam Irradiation

For the PMA 76-28 (Figure 5), the initial showed certain cracking, forming a plate-like structure on the surface. The 'bee' structures were barely visible in the image. The fibril structure was denser and more robust than for the straight run binder, while also being quite bumpy. For PMA 82-28 (Figure 6), the initial 'bee' structure was similar to that of the straight run binder, quite densely packed and somewhat larger. The fibrils were larger than for the straight run binder, and somewhat denser, while the fibrils retained a smooth texture. The initial image for the 88-28 binder showed (Figure 7) circular features similar to the binder with 10% SBS mixed in, indicating that this binder had been SBS modified, with the 'bee' structures being quite small (0.5-1µm). The fibril structure was the large in diameter along with being very bumpy and dense.

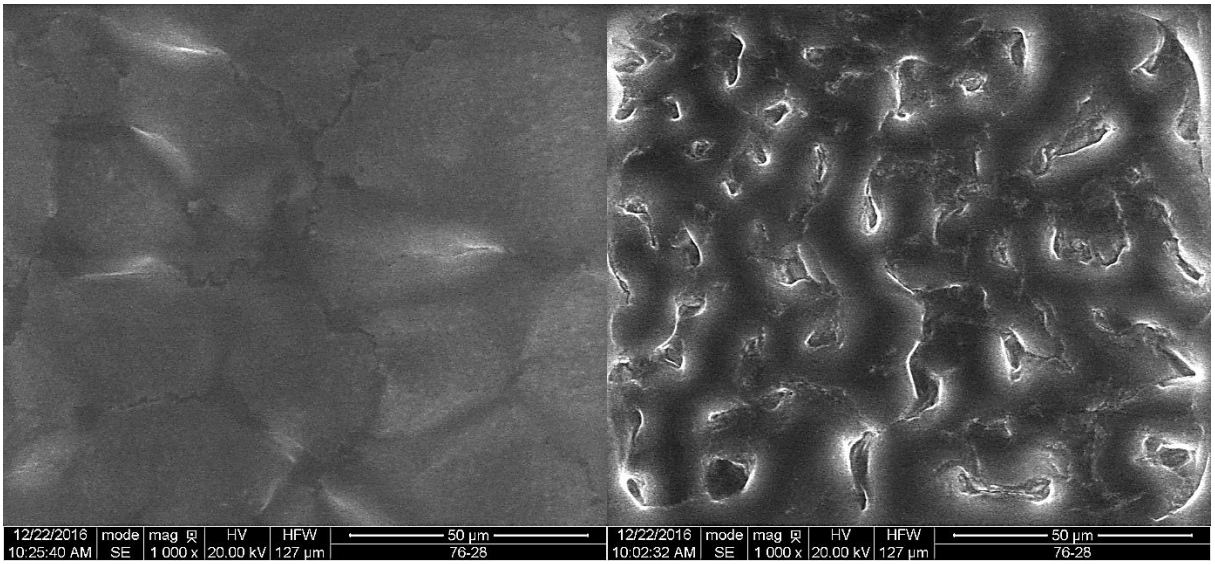

Figure 5 ESEM Images for 76-28 PMA before (left) and after (right) Electron Beam Irradiation

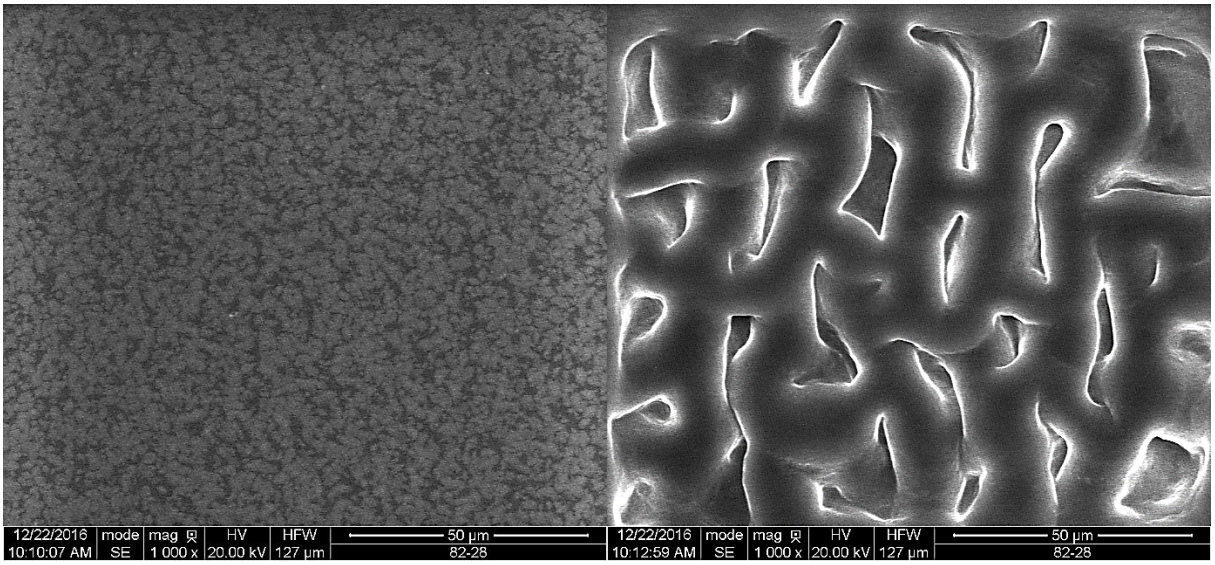

Figure 6 ESEM Images for 82-28 PMA before (left) and after (right) Electron Beam Irradiation

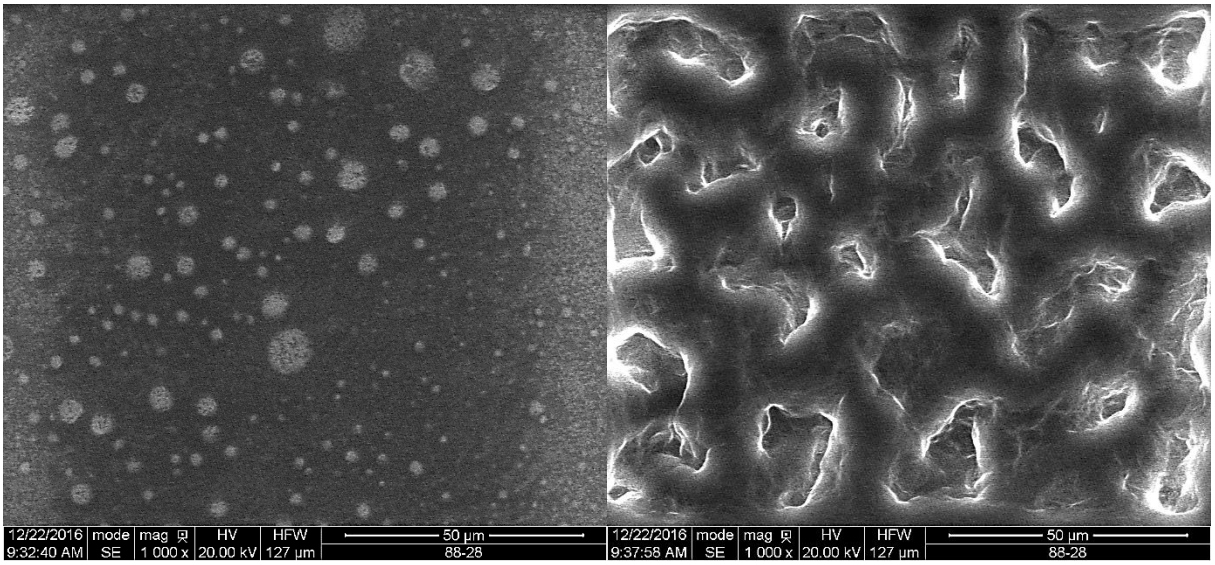

Figure 7 ESEM Images for 88-28 PMA before (left) and after (right) Electron Beam Irradiation

A summary of the binder microstructure properties revealed by the ESEM are shown in Table 1. The process for the image to form is dynamic, and reflects the properties of the binder, the times (t_1) from the start of applying the electron beam to the observed areas for the fibril structure to begin forming, and the time it takes for the fibril structure to be relatively stable (t_2). For the initial 'bee' structure, where it has been visible, the range and modes of the structures have been determined. Finally, the range and mode of the diameter of the fibrils have been determined visually, and the fibril structure was commented on in terms of density and roughness.

Table 1 Characteristics of ESEM Fibril Microstructure

Samples	Time for Structure to: (s)		Forming Time (s) Range	"Bee" Structure Length (µm)		Fibril Diameter (µm)		Fibril Characteristics	
	Start to Form	Finish Forming		Range	Mode	Range	Mode	Density	Roughness
58-28	3	40	8-12	1-3	2	8-12	10	Sparse	Smooth
58-28 + 10% SBS	6	45	8-12	1-3	2	8-12	10	Somewhat sparse	Somewhat bumpy
76-28	7	105	10-13	1-2	1	10-13	11	Fairly dense	Bumpy
82-28	22	100	12-16	1-4	3	12-16	14	Somewhat loose	Smooth
88-28	30	120	12-15	0.5-1	0.5	12-15	14	Fairly dense	Very Bumpy

The time the fibril structure takes to form in the ESEM observation will depend how easy the electron can dissipate the lighter fraction of the binder. It was found previously that this process was longer for oxidized binder (Mikhailenko et al., 2016). The results show that polymer modification of the binder significantly increases this process in terms of both the time it takes for the fibril structure to start forming, and the time it takes to stabilize. This is also an indication that this process may be related to the binder stiffness, with stiffer fibril structures taking longer to form.

The 'bee' structure found in AFM observations (Das et al., 2015) appeared for all of the binders. There was no indication that this structure was related to the presence of polymers, however. The fibril structure on the other hand, was more robust for PMAs than for the straight run binder. Additionally, the fibrils for 3 of the 4 PMAs exhibited 'bumpy' characteristics, while the fibrils for the straight rub binder were smooth. The fibril structures were also denser with PMAs, corresponding to a higher PG grade and thus, stiffness.

3.2 Image Processing and Parameters Extraction

In order to do quantitative analysis of the images, a process was implemented to extract the microscopic parameters of images, based on similar work with ESEM (Stangl et al., 2006). Boundary lines were drawn manually using Image Pro Plus in order to create a contrast between fibril and asphalt. The gray-values of asphalt were all substituted with 255 (black). Following the operations above, the original ESEM images for the five samples; as well as the transitional and final images are presented in Figures 8 to 12. With this, it was possible to quantify the length and area of the fibril part.

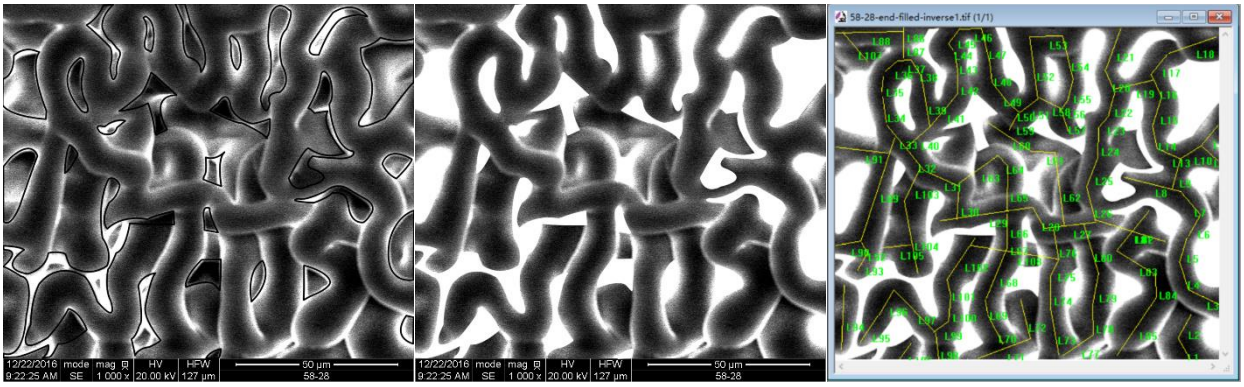

Figure 8 ESEM Image Analysis for 58-28 Straight-Run Binder

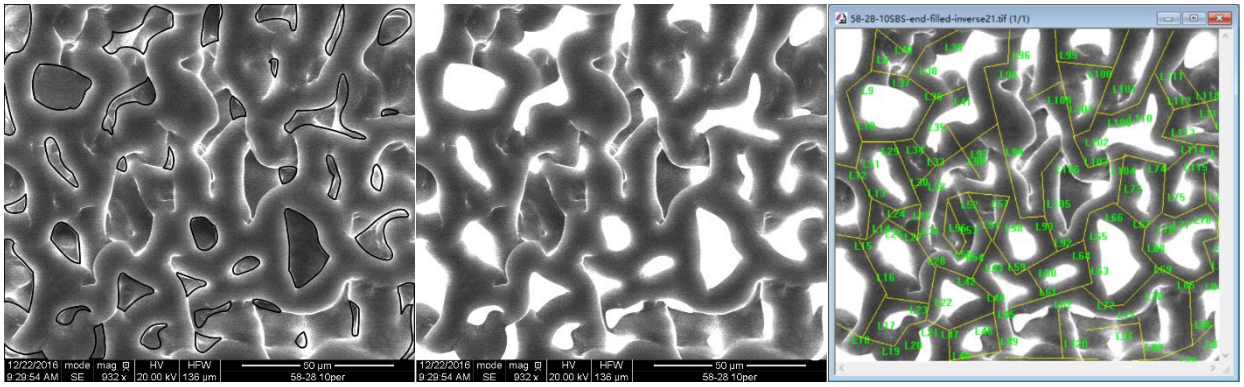

Figure 9 ESEM Image Analysis for 58-28 + 10% SBS Binder

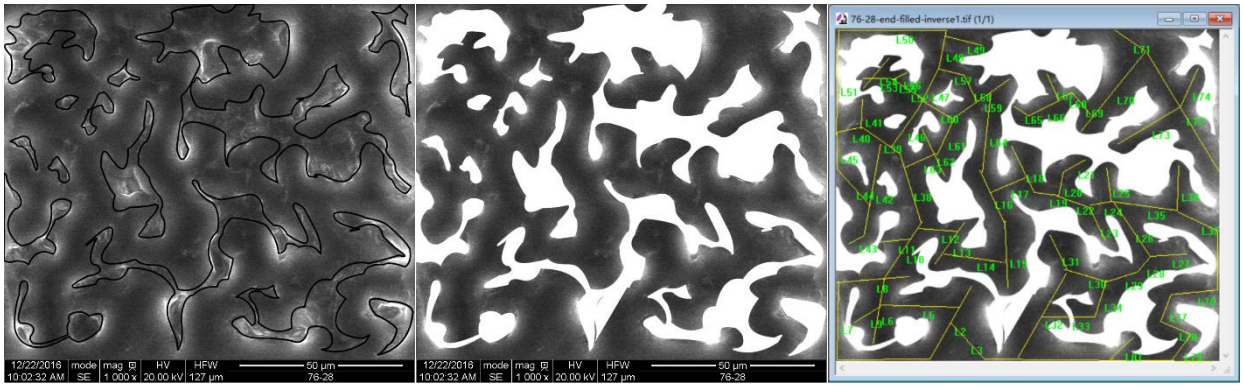

Figure 10 ESEM Image Analysis for 76-28 PMA

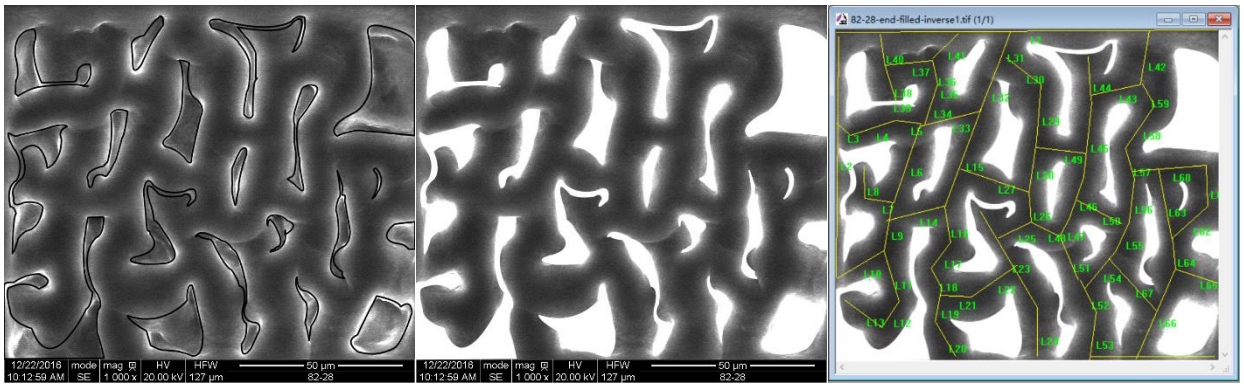

Figure 11 ESEM Image Analysis for 82-28 PMA

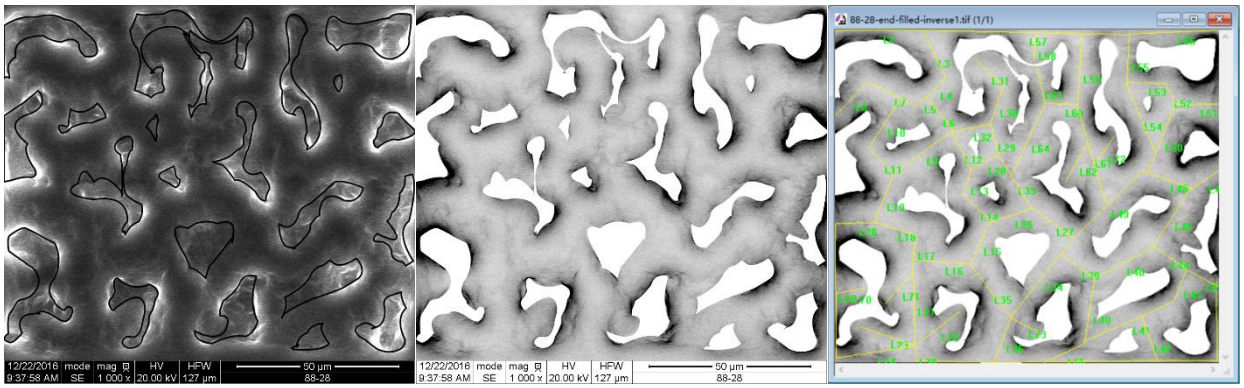

Figure 12 ESEM Image Analysis for 88-28 PMA

For comparison, the binders were ranked by different microscopic parameters as shown in Table 2. Fibril area and length showed a correlation with performance grades of the binders to some extent. In the case of PG 58-28 + 10% SBS, due to addition of the SBS polymer, the fibril area of PG 58-28 increases to a value between those for PG 88-28 and PG 82-28.

Table 2 Parameters of ESEM Fibril Microstructure

Samples	PG58-28	PG58-28 + 10% SBS	PG76-28	PG82-28	PG88-28
Fibril Percentage / %	69.98	73.94	72.04	73.50	77.68
Fibril Area / μm^2	9687.85	10236.06	9972.54	10175.15	10753.82
Fibril Length / μm	1222.05	1461.38	1332.47	1343.36	1475.27
Rank by Area	PG88-28 > PG58-28+10% SBS > PG82-28 > PG76-28 > PG58-28				
Rank by Length	PG88-28 > PG58-28+10% SBS > PG82-28 > PG76-28 > PG58-28				

However, the reliability and reproducibility cannot be guaranteed in this analysis because of limitation in sample capacity and the manual processing of the images. This analysis can hopefully contribute to more advanced ESEM analysis techniques in the future.

4. CONCLUSIONS

The conclusions of the study of PMA microstructure by ESEM are as follows:

1. PMA modification of the asphalt binder increase the fibril diameter and density of the fibril microstructure. Some PMAs also gave the fibrils a “bumpy” character.

2. The PMA modified binders had longer times for their fibril structure to form during the ESEM irradiation.

3. The SBS polymer was identified in two of the PMA samples as round elements in the ESEM image before the fibril structure appears.

4. For the quantification of the image analysis, the fibril area and fibril length were found to have some correlation with the performance grades of PMAs, with PMA modification increasing both parameters. However, more work should be done on increasing the number of images per sample and developing an automatic algorithm for their quantification.

5. REFERENCES

Baghaee Moghaddam, T., and Baaj, H. 2016. The Use of Rejuvenating Agents in Production of Recycled Hot Mix Asphalt: A Systematic Review. Construction and Building Materials 114: 805–16.

Becker, Y., Méndez M., and Rodríguez, Y. 2001. Polymer Modified Asphalt. Vision Tecnologica, 39–50.

Cortizo, M., Larsen, D., Bianchetto, H., and Alessandrini, J. 2004. Effect of the Thermal Degradation of SBS Copolymers during the Ageing of Modified Asphalts. Polymer Degradation and Stability 86 (2): 275–82.

Danilatos, G. D. 1993. Bibliography of Environmental Scanning Electron Microscopy. Microscopy Research and Technique 25 (5–6): 529–34.

Das, P., Baaj, H., Tighe, S., and Kringos N. 2015. Atomic Force Microscopy to Investigate Asphalt Binders: A State-of-the-Art Review. Road Materials and Pavement Design 0 (0): 1–26.

Dehouche, N., Kaci, M., and Mokhtar, K.A.. 2012. Influence of Thermo-Oxidative Aging on Chemical Composition and Physical Properties of Polymer Modified Bitumens. Construction and Building Materials 26 (1): 350–56.

Garcia-Morales, M., Partal, P., Navarro, F.J., and Gallegos C. 2006. Effect of Waste Polymer Addition on the Rheology of Modified Bitumen. Fuel 85 (7): 936–943.

Gaskin, J. 2013. On Bitumen Microstructure and the Effects of Crack Healing. PhD Thesis, University of Nottingham.

Kou, C., Kang, A., and Zhang, W. 2015. Methods to Prepare Polymer Modified Bitumen Samples for Morphological Observation. Construction and Building Materials 81: 93–100.

Mazumder, M., Kim, H., and Lee, S-J. 2016. Performance Properties of Polymer Modified Asphalt Binders Containing Wax Additives. International Journal of Pavement Research and Technology 9 (2): 128–39.

Mikhailenko, P. 2015. Valorisation of by-Products and Products from Agro-Industry for the Development of Release and Rejuvenating Agents for Bituminous Materials. PhD Thesis, Universite Paul Sabatier, Toulouse III.

Mikhailenko, P., Kadhim, H., and Baaj, H. 2016. Observation of Asphalt Binder Microstructure with ESEM. 2016 Transportation Association of Canada Conference, Toronto, Canada.

Mouillet, V., Lamontagne, J., Durrieu, F., Planche, J-P., and Lapalu, L. 2008. Infrared Microscopy Investigation of Oxidation and Phase Evolution in Bitumen Modified with Polymers. Fuel 87 (7): 1270–80.

Navarro, F.J., Partal, P, Martínez-Boza, F., and Gallegos, C. 2005. Effect of Composition and Processing on the Linear Viscoelasticity of Synthetic Binders. European Polymer Journal 41 (6): 1429–38.

Puente-Lee, I., Schabes-Retchkiman, P.S., Rojas-Garcia, J., Rios-Guerrero, L., and Herrera-Najera, R. 2003. Morphology Of SBS-Modified Asphalt Using Low Vacuum SEM. Microscopy and Microanalysis 9 (Supplement S02): 446–47.

Rozeveld, S., Shin, E., Bhurke, A., France, L., and Drzal, L. 1997. Network Morphology of Straight and Polymer Modified Asphalt Cements. Microscopy Research and Technique 38 (5): 529–543.

Stangl, K., Jager, A., and Lackner, R. 2006. Microstructure-Based Identification of Bitumen Performance. Road Materials and Pavement Design: An International Journal 7: 111–42.

Tarefder, R. A., and Arifuzzaman, M. 2011. A Study of Moisture Damage in Plastomeric Polymer Modified Asphalt Binder Using Functionalized AFM Tips. Journal of Systemics, Cybernetics and Informatics 9 (5): 1–12.

Yildirim, Y. 2007. Polymer Modified Asphalt Binders. Construction and Building Materials 21 (1): 66–72.